

Ultrafast spin-dynamics in half-metallic CrO₂ thin films

Qiang Zhang and A. V. Nurmikko

Division of Engineering and Department of Physics, Brown University, Providence, Rhode Island 02912, USA

G. X. Miao and G. Xiao

Department of Physics, Brown University, Providence, Rhode Island 02912, USA

A. Gupta

MINT Center, Department of Chemistry, Chemical and Biological Engineering, University of Alabama, Tuscaloosa, Alabama 35487, USA

(Received 7 March 2006; revised manuscript received 12 June 2006; published 16 August 2006)

Transient magneto-optic Kerr effect measurement utilizing ultrafast laser pulse excitation and detection method has been performed to study the spin dynamics in epitaxial CrO₂ film. Different microscopic contributions leading to incoherent spin thermalization and relaxation on distinct time scales have been identified in an extended three-temperature model (3TM), by taking into account the nonthermal electrons. Interestingly, the spins and thermalized electrons seemed to have been decoupled in these measurements, which could be attributed to the half-metallic nature of the material.

DOI: [10.1103/PhysRevB.74.064414](https://doi.org/10.1103/PhysRevB.74.064414)

PACS number(s): 75.40.Gb

I. INTRODUCTION

A key contemporary area of research in today's ferromagnetism is the study of dynamics of spin systems on ultrafast time scales, induced by their interplay with short optical pulses. Among several unique phenomena¹⁻³ that have been discovered, ultrafast demagnetization¹ describes the perturbations on the long-range order of the ground state of the many-electron system, created by short laser pulse excitations in ferromagnetic metals. Such experiments enable access to information about the fundamental interactions between the spins and the electron-lattice systems, especially their characteristic time scales. Work in conventional transition metals^{1,4} has revealed that the demagnetization process occurs at picosecond time scale or even shorter, indicating the complete dominance of the interaction between the spins and energetic electrons in comparison with spin-lattice interaction. However, comparable work in half-metallic ferromagnets⁵ is sparse, whose distinguishing characteristics is the presence of a highly spin polarized electron gas in the vicinity of the Fermi level. It has been suggested⁶ that this unique property of half-metal might lead to distinctly different spin dynamics.

The availability of high-quality single-crystal CrO₂ film has stimulated extensive study of this material in the last few years and it is probably the best-studied half-metal so far. Electronic band structure calculations^{7,8} have indicated the half metallic nature of CrO₂. Convincing experimental evidence has come from low-temperature superconducting point-contact measurement⁹ and spin-polarized photoemission spectroscopy at room temperature¹⁰ which both have yielded a very high spin polarization of $\geq 95\%$ in CrO₂. Spin dynamics in photoexcited CrO₂, however, remain largely unexplored. In this paper, we present a study of optically induced ultrafast spin dynamics in epitaxial CrO₂ film. The half metallicity of CrO₂ enables clear isolation and identification of each microscopic contribution to the spin thermalization process in the context of an extended three-

temperature model. Our key result is that the vanishing minority spin density of states (DOS) at the Fermi level in CrO₂ can greatly suppress the rate of spin-flip scattering within the nonequilibrium electron gas.

II. EXPERIMENTAL SECTION

The single crystal CrO₂ films were epitaxially grown on (100) single crystal TiO₂ substrates by chemical vapor deposition (CVD) method,¹¹ with typical thickness of 3000 Å. Their dynamics was measured by employing the transient magneto-optic Kerr effect (TMOKE), whose experimental configuration was described in Ref. 12. In the present work, excitation pulses ("pump") from a mode-locked Ti:sapphire laser ($\tau_p = 120$ fs) were directed normal to the sample and absorbed within the CrO₂ layer, at a pump fluence of about 20–200 $\mu\text{J}/\text{cm}^2$. Excitation at both 800 nm and 400 nm was used as described below. The optically induced changes in the magnetization were extracted from the measurement of transient changes in the (longitudinal) magneto-optic Kerr ellipticity in the CrO₂ film, labeled below as $\Delta\phi''(t)$, by using time-delayed weak pulses ("probe") in the near infrared ($\hbar\omega = 1.55$ eV). The Kerr instrumentation employed a polarization-sensitive optical bridge based on a Wollaston prism and a low-noise differential detector. To compensate for the relatively large third order nonlinear (electronic) optical anisotropy effect, which is typically present in metals, the experimental data were collected while applying a periodic external saturation magnetic field to the sample in opposite directions along the easy axis. The TMOKE signal, which exhibits strong magnetic field dependence, was isolated and measured by an additional lock-in amplifier in this double modulation scheme.

III. RESULTS AND DISCUSSION

The experimental results of transient magneto-optic Kerr ellipticity $\Delta\phi''(t)/\phi''$ of the CrO₂ thin films, measured from

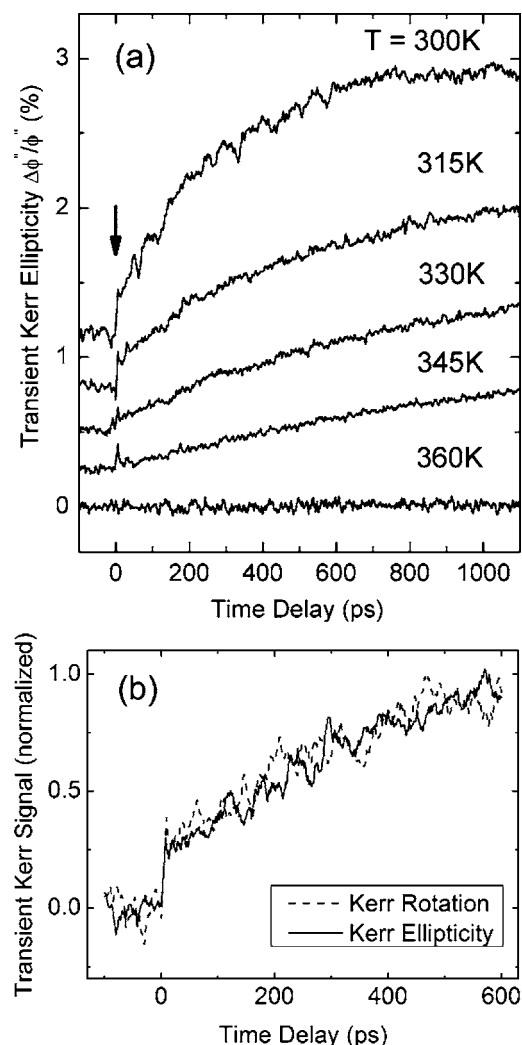


FIG. 1. (a) Temperature dependence of the transient Kerr ellipticity $\Delta\phi''/\phi''$ measurement in CrO_2 film. The temperature was varied from room temperature (300 K) toward the Curie temperature T_c (~ 390 K) of the sample. It was found that the signal amplitude dropped below the noise level when temperature was beyond 360 K. The curves are vertically displaced for clarity. The arrow indicates the occurrence of the photoexcitation. (b) Comparison of normalized transient Kerr ellipticity (solid) and transient Kerr rotation (dashed) in CrO_2 film at $T=300$ K.

$T=300$ K up to $T=360$ K toward the Curie temperature of the material at $T_c=390$ K, are illustrated in Fig. 1(a). The pump pulse was incident at the film at time $t=0$. For reference, we also measured the transient differential reflection $\Delta R(t)$, dominated by the third order nonlinear optical response and not shown explicitly here. The pump wavelength was set initially to 800 nm, for which the corresponding photon energy ($\hbar\omega=1.55$ eV) is expected to lie below the minority spin gap Δ (~ 1.8 eV), but well above the spin-flip gap Δ_{sf} (a few tenths of eV).⁵ Hence the optically induced transitions are mostly confined in the majority spin t_{2g} band¹³ according to the dipole transition selection rules. The relationship between the transient Kerr ellipticity and spin dynamics arises as follows: the signal strength of $\Delta\phi''(t)$ is proportional to the pump-induced amplitude modulation of

magnetization in the CrO_2 thin film. Thus, a larger transient Kerr ellipticity signal is directly indicative of the creation of a more highly disordered spin population, i.e., a higher spin temperature.

For the sake of verifying that the measured transient Kerr ellipticity was a true manifestation of spin dynamic behavior, transient Kerr rotation was measured as well. In the past, questions have been raised about the validity of interpreting TMOKE signal by purely spin motion at short time scales. A major concern is the influence of variation in refractive index of the magnetic medium to TMOKE through time-modulated Fresnel factor in the magneto-optic Kerr formulism,¹⁴ hence leading to a nonmagnetic contribution to the TMOKE signal. However, we note that in our experiment, the relative Kerr ellipticity changes ($\Delta\phi''/\phi'' \sim 0.1\% - 1\%$) was of comparable magnitude or larger than those in reflection ($\Delta R/R \sim 0.1\%$), further characterized by distinct temporal behaviors as described in the following of this paper. More importantly, Koopmans *et al.*¹⁵ has proposed and demonstrated a method to examine the correlation between TMOKE signals and spin dynamics by comparing the transient Kerr rotation and Kerr ellipticity collected under similar experimental configuration. An example of such comparison is displayed in Fig. 1(b) at a given temperature of 300 K. The resemblance of Kerr rotation and Kerr ellipticity traces after normalization strongly supports that they are indeed dominated by spin dynamics contribution at the time scale shown in the graph.

The data in Fig. 1 suggests that the spin dynamic behavior in CrO_2 is distinctly different from previous measurements in conventional transition metals [e.g., Ni (Ref. 1) and CoPt_3 (Ref. 4)]. Both fast and slow components are present in the traces. The slow component, occurring on a time scale of hundreds of picoseconds, gives a direct reading of the completion in the spin thermalization process. As seen here through the transient Kerr ellipticity, it increased exponentially as a function of time after the impulse of excitation and eventually reached saturation upon thermalization with electron and lattice system. Similar spin dynamic behavior has been observed in other transitional metal oxides.^{16,17} This slow component is believed to originate here dominantly from spin-lattice interaction, as opposed to electron-magnon scattering, due to its temperature dependence. Experimentally, we found that the thermalization time τ_{th} of spins, extracted from Fig. 1, slowed down as the temperature was raised, from 375 ps at $T=300$ K to 1140 ps at $T=345$ K. Beyond $T=360$ K, the signal amplitude was too small to be detected. This behavior can be understood in a three-temperature model for the spin, electron, and lattice degrees of freedom,¹ where the thermalization time τ_{th} of spins is related to the spin specific heat c_s , lattice specific heat c_l and the coupling strength g between spin and electron-lattice as $\tau_{th} \approx c_s c_l / [(c_s + c_l)g]$. In the mean field approximation, the temperature dependent c_s is given as $c_s(T) = -\alpha \frac{\partial M^2}{\partial T}$.¹⁸ Here, M is the measured spontaneous magnetization as a function of temperature and $\alpha = 3SRT_c / [2(S+1)M(0)^2]$ is a constant, where S is the average spin number ($S=2$ for CrO_2) and $M(0)$ is the saturated magnetization at low temperature. We have plotted the calculated $c_s c_l / (c_s + c_l)$ and experimentally measured τ_{th} against temperature in Fig. 2.

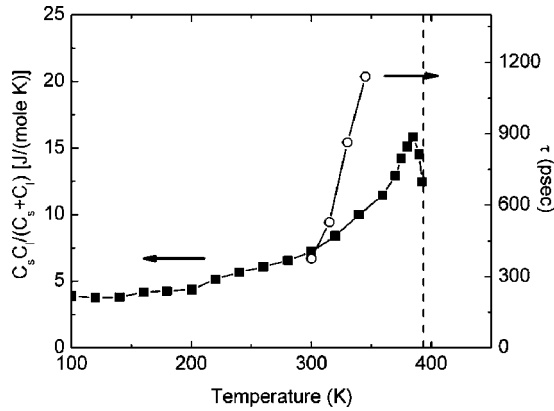


FIG. 2. Temperature dependence of effective specific heat $c_s c_l / (c_s + c_l)$ of CrO_2 (square). c_s was derived from $M(T)$ data based on mean field theory and c_l was calculated in Debye model. The measured spin thermalization time τ (circle) are also shown for comparison. The Curie temperature of CrO_2 film is marked by the dashed line.

In Fig. 2, the calculated $c_s c_l / (c_s + c_l)$ increases with temperature and peaks slightly below T_c , followed by a sudden drop. In the temperature range of interest, the measured τ_{th} varied faster than $c_s c_l / (c_s + c_l)$, by almost a factor of 2 from 300 K to 345 K, indicating that the coupling strength g was also likely to be a function of temperature. This observation is in contrast to the experimental result in perovskites manganites,¹⁹ where g displayed no strong temperature dependence. Here, the temperature dependence of g gives strong clues to its identity. According to Hübner's calculation,²⁰ single electron spin-flip rate via a Raman process in spin-lattice interaction is proportional to the magnetocrystalline anisotropy energy, which is known to exhibit similar temperature behavior. On the contrary, the electron-magnon scattering rate, as given by Campbell and Fert,²¹ increases quadratically with T , inconsistent with the observa-

tion here. Hence, we attribute the origin of the observed slow component of spin dynamics mainly to the spin-lattice interaction.

The second, fast component present in the data of Fig. 1 is a steplike increase in transient ellipticity contrast almost immediately upon pump pulse excitation, which has been largely overlooked in previous ultrafast optical studies.^{6,17} The amplitude of this steplike change in $\Delta\phi''(t)$ was relatively small, but clearly discernable. We have further measured its dependence on the polarization of the pump light and found a correlation between the step amplitude and the pump polarization when it was switched between the right-circular (RCP) and the left-circular (LCP) polarization states. In contrast, a pump-probe measurement of transient differential reflection (TR) yielded no distinction between the RCP and LCP excitations, indicating an operative selection rule for pump polarization which affects only the off-diagonal elements of the dielectric tensor, while not the diagonal ones. The result again suggests that the steplike feature in $\Delta\phi''(t)$ is associated with an initial rapid magnetization change in the CrO_2 thin film.

As far as the microscopic origin of the fast component is concerned, Zhang *et al.*²² proposed that the cooperation of laser optical field and spin-orbit coupling could lead to an extremely fast modulation of the magnetization moment by mixing the spin singlet and triplet state. However, against this explanation, we found that the TMOKE contrast generated upon photoexcitation occurs on a time scale (~ 1 ps) much longer than the laser pulse width (120 fs). As illustrated in Fig. 3 with a higher temporal resolution scan in the vicinity of pump pulse excitation (pump wavelength was set to 400 nm for better signal to noise ratio), we noticed that the TMOKE contrast rising edge lagged behind the corresponding TR trace. Hence, an electron-spin interaction nature of the fast component is suggested.

The presence of a fast component followed by a slow component drifting away further from the equilibrium point,

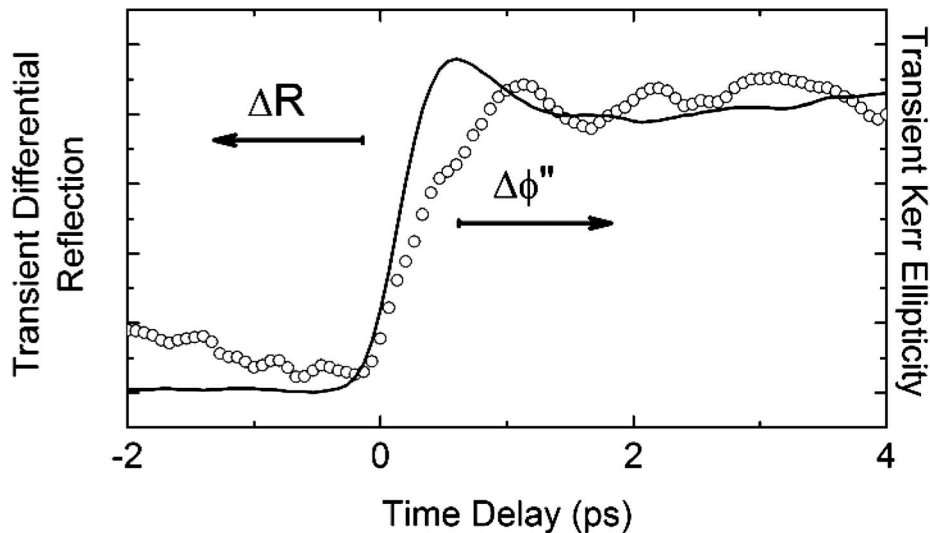


FIG. 3. High temporal resolution traces of transient Kerr ellipticity (circle) and transient differential reflection (solid line) of CrO_2 upon photoexcitation when the pump wavelength was set to 400 nm.

however, is clearly beyond the reach of conventional three-temperature model, which assumes that electron, spin and phonon systems are always in their internally thermalized states. To explain this phenomenon, one has to turn to an extended 3TM by taking into account the contribution of nonthermal electrons and is expressed as

$$\begin{aligned} \frac{\partial N}{\partial t} &= -\alpha N - \beta N - \eta N + P(t), \\ c_e(T_e) \frac{\partial T_e}{\partial t} &= -g_{el}(T_e - T_l) - g_{es}(T_e - T_s) + \alpha N, \\ c_s(T_s) \frac{\partial T_s}{\partial t} &= -g_{es}(T_s - T_e) - g_{sl}(T_s - T_l) + \eta N, \\ c_l(T_l) \frac{\partial T_l}{\partial t} &= -g_{el}(T_l - T_e) - g_{sl}(T_l - T_s) + \beta N. \end{aligned} \quad (1)$$

Here, T_e, T_l, T_s are the temperatures of the electron, lattice and spin systems, respectively. g_{el}, g_{es}, g_{sl} are their mutual interaction terms. The quantity N stands for the energy density stored in the nonthermalized part of distribution, α is the electron gas heating rate, and $\beta = g_{el}/c_e$ is the electron-phonon heating rate. The driving term $P(t)$ describes the heat source. Compared to the conventional 3TM, the interaction term η between nonthermal electrons and spins is now included. We have conducted a simulation based on extended 3TM with the following parameters for CrO_2 : the electron specific heat was obtained from $c_e(T_e) = \gamma T_e$ with $\gamma = 7 \text{ mJ K}^{-2}$,⁸ the lattice specific heat was calculated in Debye model with $\Theta_D = 593 \text{ K}$,⁵ and the spin specific heat was calculated from experimental $M(T)$ values. The interaction terms g_{el}, g_{sl} and heating rate α, η were fitting parameters and taken to be constant in the temperature range of interest for simplicity. In addition, the electron-spin interaction was assumed to be negligible, as $g_{es} \approx 0$. The heat diffusion into the substrate was also taken into account [not shown in (1)]. The details of the simulation results at $T = 300 \text{ K}$ are summarized in Fig. 4.

In Fig. 4(a), the transient temperature changes in electron, lattice and spin systems following photoexcitation are shown, together with the variation of energy density of the nonthermal electrons. The simulation results indicate that electrons and phonons will reach their thermal equilibrium within three picoseconds, while it takes much longer for spins to thermalize because of the inefficient energy transfer between the spin and electron-lattice system, as shown in Fig. 4(b). The more efficient process for spin relaxation, due to nonthermal electron spin-flip scattering, is a “window of opportunity” available for a short time (comparable to the lifetime of nonthermal electrons), which is experimentally observed to give rise to the step feature at $t = 0$ with a rise time of $\sim 1 \text{ ps}$. Thereafter the spin-lattice relaxation will dominate the thermalization of the spin system. Returning to Fig. 4(b), we can see that the experimentally measured transient Kerr ellipticity in CrO_2 has been faithfully reproduced in the transient spin temperature described by the extended 3TM. This result underscores that the vanishingly small g_{es}

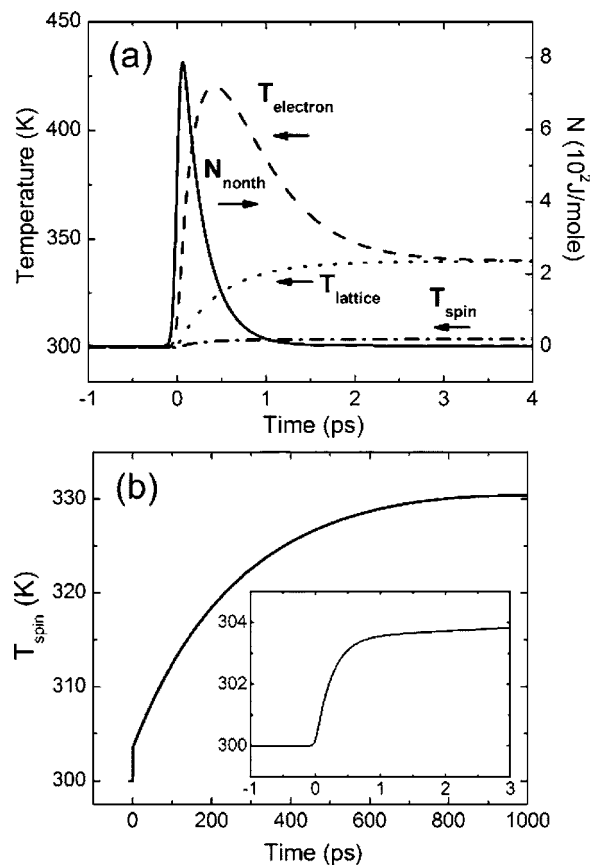


FIG. 4. Simulation of temperature changes in CrO_2 after laser pulse excitation in an extended 3TM model. (a) Temperature changes in electron (dashed), lattice (dotted), spin (dash-dot) and nonthermal electron energy density (solid) (b) Temperature in spin system alone, a zoom-in view of the first few picoseconds is shown in the inset.

term is responsible for the overall shape of the curve. Here, the half metalliticity of the material appears to play an important role. The fact that only nonthermal electrons but not thermalized electrons undergo spin flip suggests an extremely small minority spin DOS near the Fermi surface. As a result, the electron relaxation channel via single-magnon scattering is prohibited. Even though higher order terms without the requirement of involvement of spin-flip event (e.g., two-magnon scattering) may still exist, their scattering rates are expected to be much lower than the electron-phonon scattering rate. An interesting issue is how and why is the spin-lattice interaction channel active in terms of a microscopic mechanism. It is known that spin-lattice interaction originates from the fluctuation of the crystal and spin-orbit coupling. We speculate that the crystal field fluctuation might induce changes in local band structure and eventually cause local spins to flip collectively and form domains, which is expected to occur on $\sim 100 \text{ ps}$ time scale.

To further investigate the contribution of nonthermal electrons to the spin thermalization, we have compared the spin dynamics of CrO_2 under photoexcitation at two different pump wavelengths. In this measurement, we fix the probe wavelength at 800 nm and compare the TMOKE response for the pump wavelength at 800 nm ($\hbar\omega = 1.55 \text{ eV}$) and

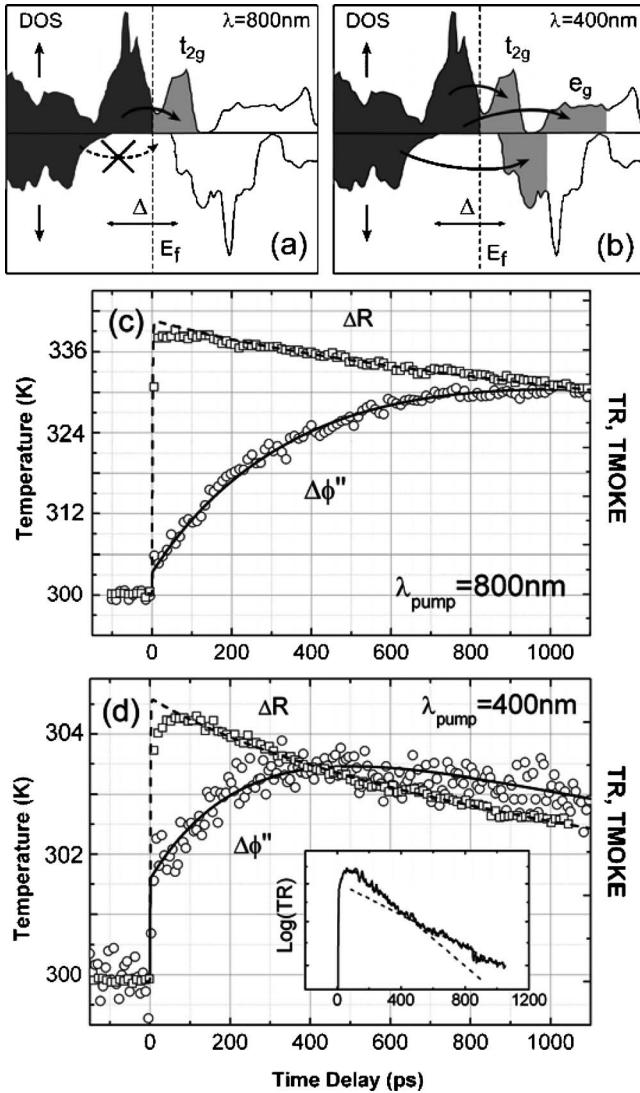


FIG. 5. (a),(b) Illustration of accessible photoexcitation and electron relaxation within the density of state of CrO_2 , with pump photon energy $\hbar\omega$ below ($\lambda_{\text{pump}}=800$ nm) and above ($\lambda_{\text{pump}}=400$ nm) the minority spin gap Δ respectively. (c),(d) Corresponding TMOKE (circle) and TR (square) measurement results. The TMOKE and TR traces are normalized such that a direct comparison with simulated spin (solid) and lattice (dashed) temperatures can be achieved. The inset in (d) plots TR in logarithmic scale.

400 nm ($\hbar\omega=3.1$ eV), which corresponds to photon energies below and above the spin gap Δ , respectively.

In Fig. 5, we connect the spin-polarized density of states (DOS) with the wavelength dependent excitation data. The DOS profiles of Figs. 5(a) and 5(b) are acquired from Ref. 8 and are used here for qualitative purposes. With excitation at $\lambda_{\text{pump}}=800$ nm, the dipole transition selection rules allow photoexcitation only within the majority spin population, as shown in Fig. 5(a). During the relaxation of these nonthermal electrons, it is anticipated that the electron-electron and electron-phonon scattering will dominate, even though there is a finite chance for the electrons to flip their spins via electron-magnon interaction (note prior commentary above). By contrast, in Fig. 5(b) when $\lambda_{\text{pump}}=400$ nm, two additional

excitation channels open up: (i) majority spin electrons can be excited into the higher energy e_g band, and (ii) the interband transition across the minority spin gap is now accessible. It follows that the chances for the photoexcited electrons to flip their spin are greatly increased. It is also worth emphasizing that it is unlikely that the minority spin electrons can relax back to vicinity of the Fermi surface without interacting with magnons. In such a picture, employing a larger pump photon energy will lead to a greatly enhanced energy transfer between the nonthermal electrons and spins during the initial stage of thermalization.

The above arguments have been confirmed by the experimental results in Figs. 5(c) and 5(d), where both TMOKE [$\Delta\phi''(t)$] and TR [$\Delta R(t)$] traces are shown. The traces are carefully normalized so that a direct comparison to the simulated temperatures of spin and lattice systems can be performed. To accomplish this, the TMOKE signal, representing magnetization variation, has been translated into spin temperature change according to the spontaneous magnetization curve. And in the perturbative regime, the TR signal can be regarded to be proportional to the lattice temperature in the temporal range of interest as depicted in the figure. As already discussed in connection with Fig. 4(b), a finite and abrupt temperature increase in the spin system immediately after the photoexcitation was observed when $\lambda_{\text{pump}}=800$ nm [Fig. 5(c)], followed by a relatively slow thermalization process occurring at 1 ns time scale. When $\lambda_{\text{pump}}=400$ nm [Fig. 5(d)], however, the enhanced energy transfer with nonthermal electrons leads to a much larger spin initial temperature jump. As a result, even though the subsequent thermalization rate with the lattice system is about the same as before, the thermal equilibrium with the lattice can be achieved more quickly, within about 400 ps. Fitting results suggested that the spin heating rate η due to nonthermal electrons increased by almost five times to $\eta=1/8$ ps $^{-1}$ when the wavelength was shortened from 800 nm to 400 nm. After thermalization, the thin CrO_2 film macroscopic system cools by heat diffusion. In fact, careful examination of the TR trace shows a slight change in the decay constant before and after the thermalization point, as highlighted in the logarithmic plot in the inset of Fig. 5(d) by the two intersecting straight lines.

IV. CONCLUSION

In summary, transient magneto-optic Kerr measurements were conducted to study the spin dynamics in photoexcited epitaxial CrO_2 thin films, to develop understanding of the relaxation processes in this half-metallic system. We find experimentally two distinct processes, operating on vastly different time scales, which dictate the spin relaxation dynamics. By examining the transient Kerr data in terms of dependence on pump wavelength, pump polarization, and temperature, we attribute the slow components on $\sim 10^2$ ps time scale to be dominated by spin-lattice relaxation. The fast component which occurs nearly instantaneously with photoexcitation has been described as the nonthermal electron contribution in an extended three-temperature model. Experiment and model suggest a vanishingly small interac-

tion strength between thermalized electrons and spins which we believe to be a distinguishing indication of the half-metallic nature of the material. Our measurement results suggest that the local exchange splitting and the energy gap in

minority spins survive at elevated temperatures up to near the Curie temperature, indicating that the exchange coupling between conducting and localized electrons in CrO_2 remains in the strong coupling regime.

-
- ¹E. Beaurepaire, J.-C. Merle, A. Daunois, and J.-Y. Bigot, *Phys. Rev. Lett.* **76**, 4250 (1996).
- ²G. Ju, A. V. Nurmikko, R. F. C. Farrow, R. F. Marks, M. J. Carey, and B. A. Gurney, *Phys. Rev. Lett.* **82**, 3705 (1999).
- ³G. Ju, J. Hohlfeld, B. Bergman, R. J. M. van deVeerdonk, O. N. Mryasov, J.-Y. Kim, X. Wu, D. Weller, and B. Koopmans, *Phys. Rev. Lett.* **93**, 197403 (2004).
- ⁴E. Beaurepaire, M. Maret, V. Halté, J.-C. Merle, A. Daunois, and J.-Y. Bigot, *Phys. Rev. B* **58**, 12134 (1998).
- ⁵J. M. D. Coey and M. Venkatesan, *J. Appl. Phys.* **91**, 8345 (2002).
- ⁶T. Kise, T. Ogasawara, M. Ashida, Y. Tomioka, Y. Tokura, and M. Kuwata-Gonokami, *Phys. Rev. Lett.* **85**, 1986 (2000).
- ⁷K. Schwarz, *J. Phys. F: Met. Phys.* **16**, L211 (1986).
- ⁸S. P. Lewis, P. B. Allen, and T. Sasaki, *Phys. Rev. B* **55**, 10253 (1997).
- ⁹Y. Ji, G. J. Strijkers, F. Y. Yang, C. L. Chien, J. M. Byers, A. Anguelouch, G. Xiao, and A. Gupta, *Phys. Rev. Lett.* **86**, 5585 (2001).
- ¹⁰Y. S. Dedkov, M. Fonine, C. König, U. Rüdiger, G. Güntherodt, S. Senz, and D. Hesse, *Appl. Phys. Lett.* **80**, 4181 (2002).
- ¹¹X. W. Li, A. Gupta, T. T. McGuire, P. R. Duncombe, and G. Xiao, *J. Appl. Phys.* **85**, 5585 (1999).
- ¹²Q. Zhang, A. V. Nurmikko, A. Anguelouch, G. Xiao, and A. Gupta, *Phys. Rev. Lett.* **89**, 177402 (2002).
- ¹³I. I. Mazin, D. J. Singh, and C. Ambrosch-Draxl, *Phys. Rev. B* **59**, 411 (1999).
- ¹⁴C. Y. You and S. C. Shin, *J. Appl. Phys.* **84**, 541 (1998).
- ¹⁵B. Koopmans, M. vanKampen, J. T. Kohlhepp, and W. J. M. de Jonge, *Phys. Rev. Lett.* **85**, 844 (2000).
- ¹⁶R. D. Averitt, A. I. Lobad, C. Kwon, S. A. Trugman, V. K. Thorsmølle, and A. J. Taylor, *Phys. Rev. Lett.* **87**, 017401 (2001).
- ¹⁷T. Ogasawara, M. Matsubara, Y. Tomioka, M. Kuwata-Gonokami, H. Okamoto, and Y. Tokura, *Phys. Rev. B* **68**, 180407(R) (2003).
- ¹⁸D. H. Martin, *Magnetism in Solids* (MIT Press, Cambridge, MA, 1967).
- ¹⁹A. I. Lobad, R. D. Averitt, C. Kwon, and A. J. Taylor, *Appl. Phys. Lett.* **77**, 4025 (2000).
- ²⁰W. Hübner and K. H. Bennemann, *Phys. Rev. B* **53**, 3422 (1996).
- ²¹A. H. Morrish, in *The Physical Principles of Magnetism* (Wiley-IEEE Press, Piscataway, New Jersey, 1965), pp. 87–105.
- ²²G. P. Zhang and W. Hübner, *Phys. Rev. Lett.* **85**, 3025 (2000).